Do Phytotropins Inhibit Auxin Efflux by Impairing Vesicle Traffic?[1]

Jan Petrášek, Adriana Černá, Kateřina Schwarzerová, Miroslav Elčkner, David A. Morris[2], and Eva Zažímalová*

Institute of Experimental Botany, The Academy of Sciences of the Czech Republic, Rozvojová 135, CZ–16502 Prague 6, Czech Republic (J.P., M.E., D.A.M., E.Z.); and Department of Plant Physiology, Faculty of Science, Charles University, Viničná, CZ–12844 Prague 2, Czech Republic (J.P., A.Č., K.S.)

Phytotropins such as 1-*N*-naphthylphthalamic acid (NPA) strongly inhibit auxin efflux, but the mechanism of this inhibition remains unknown. Auxin efflux is also strongly decreased by the vesicle trafficking inhibitor brefeldin A (BFA). Using suspension-cultured interphase cells of the BY-2 tobacco (*Nicotiana tabacum* L. cv Bright-Yellow 2) cell line, we compared the effects of NPA and BFA on auxin accumulation and on the arrangement of the cytoskeleton and endoplasmic reticulum (ER). The inhibition of auxin efflux (stimulation of net accumulation) by both NPA and BFA occurred rapidly with no measurable lag. NPA had no observable effect on the arrangement of microtubules, actin filaments, or ER. Thus, its inhibitory effect on auxin efflux was not mediated by perturbation of the cytoskeletal system and ER. BFA, however, caused substantial alterations to the arrangement of actin filaments and ER, including a characteristic accumulation of actin in the perinuclear cytoplasm. Even at saturating concentrations, NPA inhibited net auxin efflux far more effectively than did BFA. Therefore, a proportion of the NPA-sensitive auxin efflux carriers may be protected from the action of BFA. Maximum inhibition of auxin efflux occurred at concentrations of NPA substantially below those previously reported to be necessary to perturb vesicle trafficking. We found no evidence to support recent suggestions that the action of auxin transport inhibitors is mediated by a general inhibition of vesicle-mediated protein traffic to the plasma membrane.

The polar transport of auxins (such as indole-3-acetic acid [IAA]) plays a crucial role in the regulation of growth and development in plants (Davies, 1995). Much experimental evidence supports the proposal by Rubery and Sheldrake (1974) and Raven (1975) that auxin transport polarity results from the differential permeabilities of each end of transporting cells to auxin anions (IAA^-) and undissociated auxin molecules (IAA; for review, see Goldsmith, 1977). IAA (a weak organic acid) is relatively lipophilic and can readily enter cells by diffusion from the more acidic extracellular space; the IAA^- anion, on the other hand, is hydrophilic and does not cross membranes easily. As a consequence, auxins tend to accumulate in plant cells by a process of "anion trapping" and exit the symplast with the intervention of transmembrane auxin anion efflux carriers (Goldsmith, 1977). There is now overwhelming evidence that the differential efflux of IAA^- anions from the two ends of auxin-transporting cells results from an asymmetric (polar) distribution of such carriers (Goldsmith, 1977; Lomax et al., 1995). Genes encoding putative auxin influx and efflux carriers have been identified from Arabidopsis and other species (for review, see Morris, 2000; Muday and DeLong, 2001; Friml and Palme, 2002). It has been shown that efflux carrier proteins, encoded by members of the *PIN* (*PIN-FORMED*) gene family, and possibly influx carriers (encoded by *AUX1*), are targeted to specific regions of the plasma membrane (PM) in auxin-transporting cells (Bennett et al., 1996; Gälweiler et al., 1998; Müller et al., 1998; Swarup et al., 2001; for review, see Friml and Palme, 2002).

Studies employing specific inhibitors of components of the polar auxin transport process have played a major role in shaping our understanding of the polar auxin transport machinery. The most widely used inhibitor of auxin efflux is 1-*N*-naphthylphthalamic acid (NPA), a well-characterized member of a group of inhibitors known as phytotropins (Katekar and Geissler, 1980; Rubery, 1990). The application of NPA to various plant tissues results in the inhibition of auxin efflux carrier activity and, as a consequence, increases auxin accumulation in cells (for review, see Morris, 2000). Although the mechanism of its inhibitory action on polar auxin transport remains obscure, it seems to be mediated by a specific, high affinity, NPA-binding protein (NBP; Sussman and Gardner, 1980; Rubery, 1990). Observations on zuc-

[1] This work was supported by the European Union, International Cooperation Copernicus (grant no. ERBIC15 CT98 0118 to E.Z.); by the Ministry of Education, Youth, and Sports of the Czech Republic (project no. LN00A081); and by the UK Royal Society and the Academy of Sciences of the Czech Republic under the European Science Exchange Scheme (grant to D.A.M.).

[2] Present address: Division of Cell Sciences, School of Biological Sciences, University of Southampton, Bassett Crescent East, Southampton SO16 7PX, UK.

* Corresponding author; e-mail eva.zazim@ueb.cas.cz; fax 420–220390–474.

Article, publication date, and citation information can be found at www.plantphysiol.org/cgi/doi/10.1104/pp.012740.

chini (*Cucurbita pepo*) hypocotyl cells have shown that the NBP is probably a peripheral membrane protein located on the cytoplasmic face of the PM and associated with the cytoskeleton (Cox and Muday, 1994; Dixon et al., 1996; Butler et al., 1998; but compare with Bernasconi et al., 1996). Protein synthesis inhibitors such as cycloheximide (CH) rapidly uncouple carrier-mediated auxin efflux and the inhibition of efflux by NPA (Morris et al., 1991). In the short term, however, CH has no effect on either the specific and saturable binding of NPA or on auxin efflux itself, suggesting that the NBP and the efflux catalyst may interact through a third, rapidly turned over protein (Morris et al., 1991; for discussion, see Morris, 2000; Luschnig, 2001). Although the identity of the NBP and its mechanism of action on auxin efflux carriers remain unknown, the Arabidopsis *tir3* (*transport inhibitor response 3*) mutant exhibits a reduced number of NPA-binding sites and a reduction in polar auxin transport (Ruegger et al., 1997). Thus, *TIR3* (renamed *BIG* by Gil et al., 2001, to reflect the unusually large size—566 kD—of the protein it encodes) may code for an NBP or may be required for NBP expression, localization, or stabilization (for discussion see Gil et al., 2001; Luschnig, 2001).

In addition to polar auxin transport inhibitors, drugs that inhibit Golgi-mediated vesicle traffic, such as brefeldin A (BFA) and monensin, also very rapidly inhibit auxin efflux carrier activity in zucchini hypocotyl tissue (Wilkinson and Morris, 1994; Morris and Robinson, 1998), and in suspension-cultured tobacco (*Nicotiana tabacum* L. cv Xanthi XHFD8) cells (Delbarre et al., 1998). They also inhibit polar auxin transport through tissue (Robinson et al., 1999). However, the time lag for inhibition of efflux carrier activity by BFA (minutes) is considerably shorter than the lag for inhibition of efflux activity by protein synthesis inhibitors (up to 2 h; Morris et al., 1991). This implies that efflux catalysts turn over very rapidly in the PM without a requirement for concurrent protein synthesis, a situation that contrasts sharply with the inhibitory action of NPA on auxin efflux, which does require concurrent protein synthesis (see above). Results of a detailed comparison of the effects of CH and BFA on efflux carrier activity revealed that efflux carrier proteins probably cycle between the PM and an unidentified intracellular compartment (Robinson et al., 1999; compare with Delbarre et al., 1998). This possibility has been strongly supported by the observation that AtPIN1, a member of a family of putative Arabidopsis auxin efflux carrier proteins (see Friml and Palme, 2002), is rapidly and reversibly internalized after BFA treatment of Arabidopsis roots (Geldner et al., 2001).

A link has been suggested recently between the inhibitory action of polar auxin transport inhibitors on auxin efflux and their inhibitory effects on the actin-dependent vesicle trafficking and cycling of efflux carrier proteins (Geldner et al., 2001). Treatment of Arabidopsis roots with the auxin transport inhibitor 2,3,5-triiodobenzoic acid (TIBA) prevented the BFA-induced internalization of the putative auxin efflux carrier AtPIN1 and prevented the traffic of internalized PIN1 to the PM after BFA washout. This would have the effect of reducing the density of carriers in the PM available for auxin efflux. The authors found similar effects of TIBA on a rapidly turned-over PM-ATPase and the *KNOLLE* gene product (a syntaxin involved in vesicle docking; see Muday and Murphy, 2002). As a consequence, a rather general action of auxin transport inhibitors on membrane-trafficking processes was suggested, rather than a specific effect on auxin efflux carriers (Geldner et al., 2001).

The site-directed traffic of auxin efflux carrier proteins involves not only the Golgi-mediated secretory system itself, but also the participation of components of the cytoskeletal system. The application of cytochalasin (an actin-depolymerizing agent) reduced polar auxin transport in maize (*Zea mays*) coleoptiles (Cande et al., 1973) and in zucchini hypocotyls (Butler et al., 1998). Moreover, cytochalasin D has been shown recently to block the cycling of PIN1 between endosomal compartments and the PM in Arabidopsis roots (Geldner et al., 2001). These observations are consistent with an important role for actin filaments (AFs) in the proper localization and function of components of the auxin efflux carrier complex (for review, see Muday, 2000; Muday and Murphy, 2002). Evidence from a careful in vitro biochemical analysis of the association between the NBP and the cytoskeleton in membrane preparations from zucchini hypocotyls indicates a strong link between NPA action and the actin cytoskeleton (Butler et al., 1998). Only treatments that stabilized F-actin (phalloidin), but not those that stabilized microtubules (MTs; taxol), increased NPA-binding activity. Furthermore, direct interaction between the high-affinity NBP and F-actin was proven by F-actin affinity chromatography in the same system (Hu et al., 2000).

The processes that regulate the cycling of the efflux carrier proteins and that direct their traffic to specific areas of the PM remain unknown, although recent observations are beginning to provide insights into possible mechanisms. Gil et al. (2001) have reported that *tir3* (see above) and *doc1* (*dark overexpression of CAB*; Li et al., 1994) are allelic mutants of a gene (*BIG*) that has significant identity with the *CAL/O* (*CALOSSIN/PUSHOVER*) gene. The product of *CAL/O* is involved in the regulation of synaptic vesicle cycling in *Drosophila melanogaster* (Richards et al., 1996). BIG (TIR3) is required for normal auxin transport in plants and is probably associated with the actin cytoskeleton (Cox and Muday, 1994; Butler et al., 1998). Because the cycling of putative auxin efflux carrier proteins involves BFA-sensitive and actin-dependent vesicle traffic to the PM (Geldner et al., 2001), BIG

may play a similar role in plants to that of CAL/O in *D. melanogaster*, and regulate this directed vesicle traffic.

The observations discussed above associate the inhibition of auxin efflux carrier activity by NPA with effects of the compound on actin-dependent and Golgi vesicle-mediated targeting of efflux carrier protein to the PM. Nevertheless, almost nothing is known about the effects (if any) of NPA or other phytotropins on the organization of components of the cytoskeleton or on the vesicle secretory system. Given the possibility that phytotropins might have a general effect on vesicle traffic to the PM and on the cycling of proteins between the PM and endosomal compartments (as suggested by Geldner et al., 2001; but see "Discussion"), some physical disruption of the secretory pathway and/or cytoskeleton might be expected to occur after the application of these compounds. However, to the best of our knowledge, no such disruption has been reported so far.

Here, we report an investigation to compare the action of BFA and NPA on both auxin accumulation and on the arrangement and structure of components of the secretory pathway and the cytoskeleton (AFs, MTs, and endoplasmic reticulum [ER]) in suspension-cultured BY-2 tobacco cells. Using a new quantitative method to study the rearrangement of AFs and the formation of actin clusters in the perinuclear region of cells, we show that although both of these compounds increase auxin accumulation by inhibiting auxin efflux, only BFA has an effect on the structure of AFs and the ER. Our observations lead us to suggest that although radial and perinuclear (but possibly not cortical) AFs and ER are required for normal auxin efflux, the inhibitory action of NPA on efflux does not involve any changes in the cytoskeleton and ER.

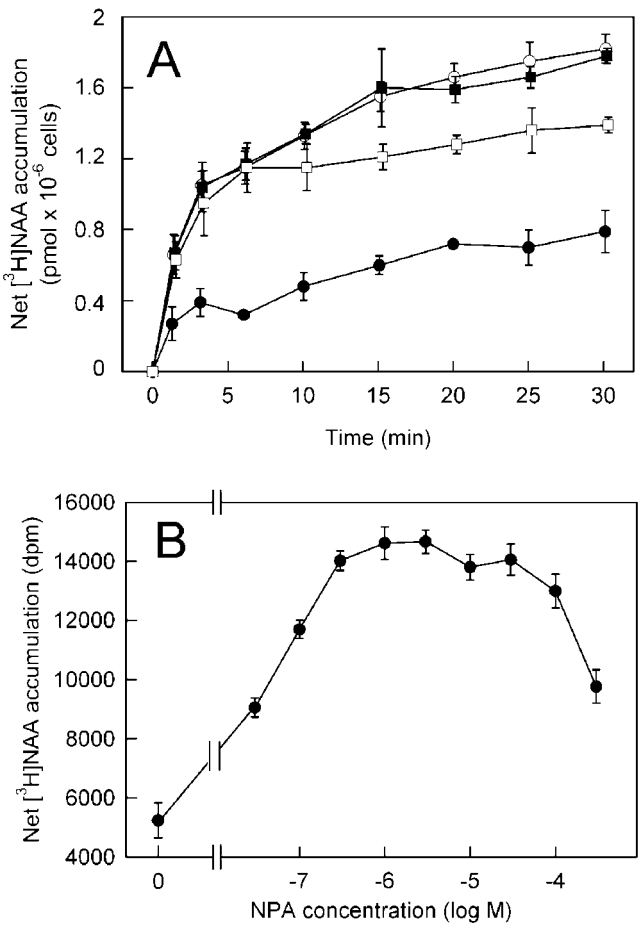

Figure 1. The effect of NPA on the net accumulation of [^{3}H]NAA (2 nM) in 2-d-old BY-2 cells. A, Time course of net [^{3}H]NAA accumulation in the absence (●, control) and in the presence of 10 μM (○), 50 μM (■), and 200 μM (□) NPA. Error bars = SEs of the mean (n = 3). B, The effect of concentration of NPA on net [^{3}H]NAA accumulation, measured over 20 min, by 2-d-old BY-2 cells. Results expressed as mean radioactivity per 0.5 mL of cell suspension (cell density 7×10^5 cells mL^{-1}). Error bars = SEs of the mean (n = 4).

RESULTS

Effects of NPA and BFA on the Accumulation of Auxin

The rate of [^{3}H]-labeled naphthalene-1-acetic acid ([^{3}H]NAA) accumulation by BY-2 cells is shown in Figures 1A and 2A. After an initial period of rapid uptake lasting 3 to 10 min depending on experiment, uptake settled to a slower, steady rate that was maintained for up to 40 min. Accumulation was extremely sensitive to NPA and was stimulated approximately 3-fold in the presence of 10 or 50 μM NPA (Fig. 1A). An NPA concentration dependence study indicated that [^{3}H]NAA accumulation was maximally stimulated by as little as 1.0 μM NPA and that the stimulatory effect of NPA began to decline rapidly at concentrations around or greater than 100 μM (Fig. 1B). Because of the greatly reduced stimulation of [^{3}H]NAA accumulation at high concentrations of NPA, possibly caused by toxic side effects not directly related to auxin efflux, the maximum concentration of NPA employed in subsequent cytological observations was restricted to 50 μM.

A similar picture emerged in the case of BFA (Fig. 2), although the maximum stimulation of [^{3}H]NAA accumulation (at between 10 and 40 μM BFA) was lower than that caused by NPA (compare Figs. 1A with 2A, and 1B with 2B). As with NPA, high concentrations of BFA (100 μM) reduced the stimulation of [^{3}H]NAA accumulation (Fig. 2B).

Over the uptake period used here, no significant metabolism of [^{3}H]NAA by BY-2 cells was detected. Apart from a small amount of label that remained at the origin in all chromatography solvents used (less than 10% of the total label recovered), the recovered ethanol-soluble radioactivity migrated as a single spot that had the same mobility on cellulose thin-layer plates as authentic [^{3}H]NAA (data not shown).

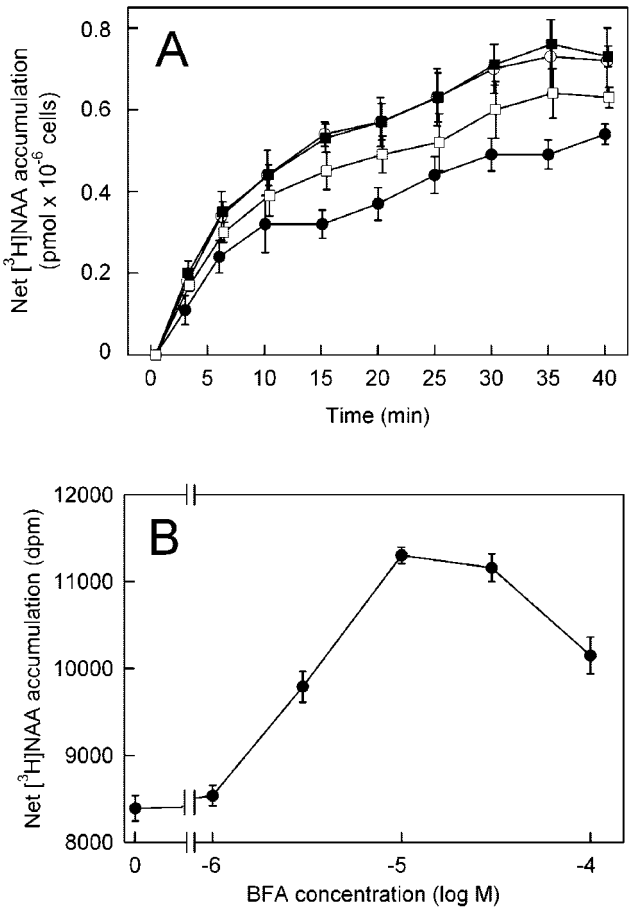

Figure 2. The effect of BFA on the net accumulation of [^{3}H]NAA (2 nM) in 2-d-old BY-2 cells. A, Time course of net [^{3}H]NAA accumulation in the absence (●, control) and in the presence of 20 μM (○), 40 μM (■), and 100 μM (□) BFA. Error bars = SEs of the mean (n = 3). B, The effect of concentration of BFA on net [^{3}H]NAA accumulation, measured over 20 min, by 2-d-old BY-2 cells. Results expressed as mean radioactivity per 0.5 mL of cell suspension (cell density 7×10^5 cells mL^{-1}). Error bars = SEs of the mean (n = 4).

Effects of BFA and NPA on AFs and MTs

To test the reaction of the cytoskeleton to the application of agents that modify polar auxin transport, the arrangement of both AFs and MTs in BFA- and NPA-treated cells was studied during a 30-min incubation period in parallel with the auxin accumulation measurements described above. Because the cell populations used to measure auxin accumulation were predominantly in interphase, we investigated the arrangement of the interphase cytoskeleton (MTs and AFs in the cortical cytoplasm and AFs in the transvacuolar strands and perinuclear region). Typical interphase BY-2 tobacco cells contained fine and transversally oriented AFs (Fig. 3A) and MTs (Fig. 3G) in the cortical cytoplasm, together with radially oriented AFs in transvacuolar strands and in the perinuclear region (Fig. 3D). There were no MTs in transvacuolar strands and around the nucleus in interphase cells (Fig. 3G). Although both NPA and BFA significantly increased auxin accumulation (Figs. 1 and 2), their effects on cytoskeleton arrangement differed considerably. Although the fine cortical AFs and MTs retained their transverse orientation after a 30-min treatment with 20 μM BFA (Fig. 3, B and H), BFA had a dramatic effect on the arrangement of the radial and perinuclear AFs (Fig. 3E). Fine AFs in the transvacuolar strands collapsed and actin became concentrated in clusters around the nucleus (Fig. 3E).

We have developed a simple procedure for the evaluation of quantitative changes in actin aggregation in the perinuclear region, utilizing image analysis software. This method is based on the fact that relative fluorescence intensities of regions with aggregated actin are very different from the background fluorescence intensities. Thus, aggregation of actin increases the degree of variation in fluorescence intensities of individual pixels in the area of interest. Full details of the procedure are described in "Materials and Methods" (see also Fig. 4). This procedure was used to evaluate the effects of BFA and it was shown that the degree of actin aggregation noticeably increased with duration of treatment (Fig. 4E). The highest BFA concentration tested (100 μM) was shown to be inhibitory for actin aggregation in the same way that it was inhibitory for auxin accumula-

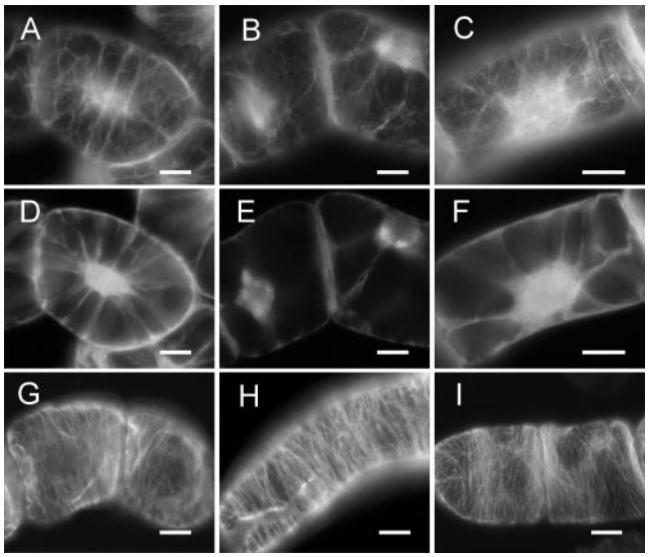

Figure 3. The effect of BFA and NPA on the arrangement of AFs and MTs in 2-d-old BY-2 cells. Control cells with fine AFs in the cortical region (A), radially oriented AFs in transvacuolar strands (D), and transversely oriented cortical MTs (G). B, E, and H, AFs and cortical MTs after 30-min incubation in 20 μM BFA. Modification of AFs staining pattern in cortical (B) and perinuclear region (E), where AFs in transvacuolar strands are "pulled down," forming clusters around the nucleus. H, Unaffected arrangement of cortical MTs. C, F, and I, AFs and cortical MTs after 30-min incubation in 50 μM NPA. Unaltered AFs staining pattern in the cortical (C) and perinuclear region (F). I, Transversally oriented cortical MTs with no obvious changes. Each image is representative of cells in the treatment specified. Approximately 1,000 cells per treatment were examined. Scale bars = 10 μm.

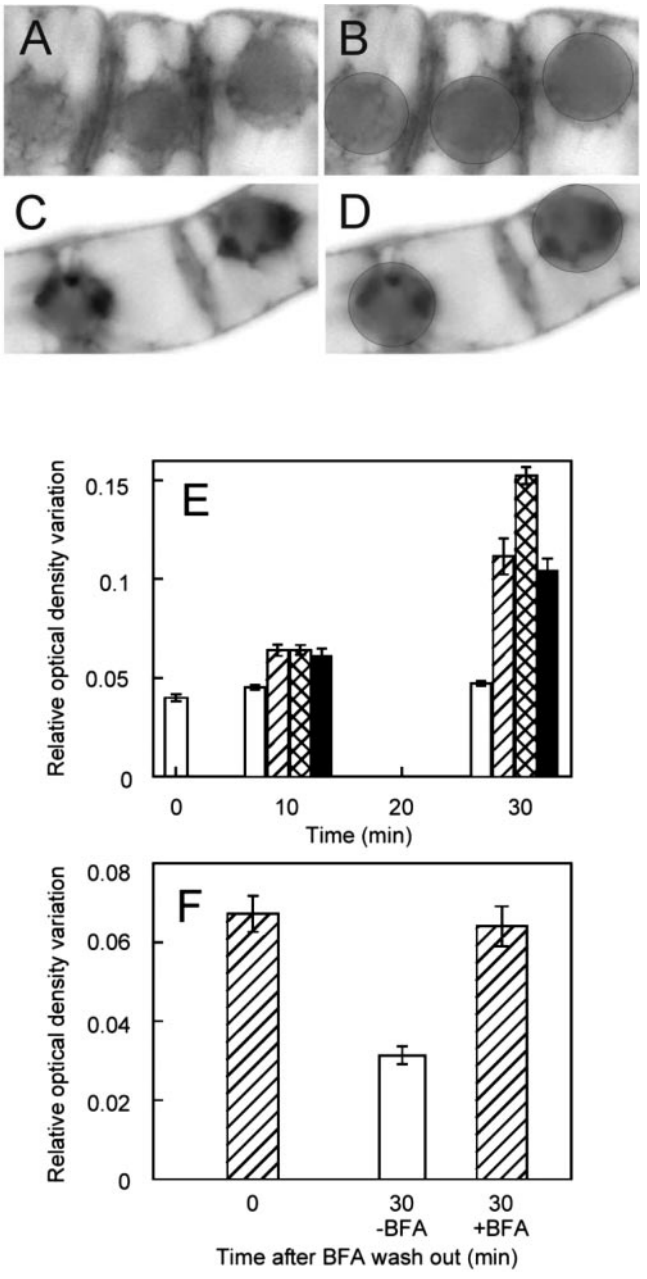

Figure 4. The quantification of BFA effect on AFs. Grabbed images of tetramethylrhodamine B isothiocyanate (TRITC)-phalloidin-stained control (A) and BFA-treated cells (C) after transformation to complementary colors. B and D, Interactively applied circular measuring frame over the perinuclear region for the measurement of the relative optical density variation (ODV) parameter. See "Materials and Methods" for details. E, Relative ODV in control (white columns) and in the presence of 20 μM (shaded columns), 40 μM (checked columns), and 100 μM (black columns) BFA. F, Relative ODV after 30-min incubation in 20 μM BFA (time 0 min, shaded column) and after washout and subsequent 30-min incubation in fresh medium without BFA (time 30 min, white column) and in the presence of 20 μM BFA in the medium (time 30 min, shaded column). Error bars = SEs of the mean (n = 10 optical fields, 30 cells assessed in each).

tion (compare Fig. 4E with 2B). The effect of BFA on AFs was reversible and 30 min after washout of BFA with fresh medium, the actin clusters disappeared and the ODV parameter decreased again to control values (Fig. 4F).

In contrast to BFA, 30 min of incubation in 50 μM NPA did not cause any changes in the arrangement of AFs in cortical region (Fig. 3C; compare with Fig. 3, A and B) as well as around the nucleus and in the transvacuolar strands (Fig. 3F; compare with Fig. 3, D and E). Correspondingly, cortical MTs were also unaffected after 30 min in 50 μM NPA (Fig. 3I; compare with Fig. 3, G and H).

The Effect of BFA and NPA on the ER

In addition to the Golgi apparatus, the plant ER has also been shown to be sensitive to BFA treatment (Henderson et al., 1994). Therefore, we investigated if the ER was also affected in cells in which BFA or NPA stimulated the accumulation of auxin. The behavior of ER in interphase cells of BY-2 after NPA or BFA treatment was followed in vivo using cells transformed with the pBIN *m-gfp5*-ER plant binary vector coding for the ER-localized fusion protein (mGFP5-ER). In exponentially growing control interphase cells, ER was present in the form of a tubular network penetrating not only the cortical layer of cytoplasm (Fig. 5A), but also the transvacuolar strands and perinuclear region (Fig. 5D). Within this network, small motile bodies were observed (video sequence can be seen at http://www.ueb.cas.cz/laboratory_of_hormonal_regulations/BFAmovies.htm). The movement of these bodies was observed over the surface of the network of ER tubules that constantly changed its orientation and pattern. Treatment of cells with 20 μM BFA for 30 min resulted in disintegration of the fine tubular network of ER, the formation of large sheets of ER, and the aggregation of the signal into a large number of bright fluorescent spots (Fig. 5B; video sequence can be seen at http://www.ueb.cas.cz/laboratory_of_hormonal_regulations/BFAmovies.htm). However, the first observable effects of BFA were clear after only 5 min (data not shown), when disintegration of the tubular network and formation of fluorescent spots started. On the other hand, even after 30 min of 20 μM BFA treatment, there were still cells with no obvious damage of ER. The accumulation of GFP fluorescence was also observed in the perinuclear region (Fig. 5E). Moreover, the movement of small motile bodies inside ER tubules decreased during a 30-min incubation in 20 μM BFA and had almost stopped by the end of that time period. Longer treatment with 20 μM BFA (7 h) resulted in the formation of large sheets of ER and intensively fluorescing bodies of irregular shape and size (data not shown).

In contrast to BFA, a 30-min incubation in 50 μM NPA had no observable effects on either ER structure

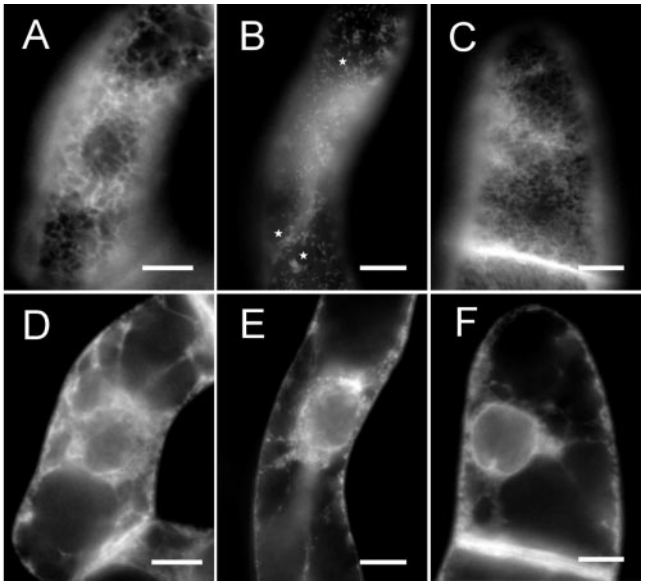

Figure 5. The effect of BFA and NPA on the arrangement of ER in 2-d-old BY-2 cells expressing mGFP5-ER. A and D, Green fluorescent protein (GFP) fluorescence in control cells. Optical cuts through cortical region (A) and perinuclear region (D). B and E, GFP fluorescence in cells after 30-min incubation in 20 μM BFA. The formation of bright fluorescent spots (B) and large sheets (B, asterisks) in the cortical layer are shown. Bright fluorescent spots in transvacuolar strands and in the perinuclear region (E). Video files showing control cells and the effect of 30-min incubation in 20 μM BFA can be seen at http://www.ueb.cas.cz/laboratory_of_hormonal_regulations/BFAmovies.htm. C and F, GFP fluorescence in cells after 30-min incubation in 50 μM NPA. Unaltered ER in the cortical (C) and perinuclear region (F). Bars = 10 μm.

or arrangement (Fig. 5, C and F); furthermore, no changes in the movement of small bodies were found.

The effects of both NPA and BFA on the cell structures examined and on auxin accumulation are summarized in Table I.

DISCUSSION

The Actions of NPA and BFA on Auxin Accumulation Differ

In suspension-cultured tobacco cells, NAA accumulation (inhibition of efflux) is controlled predominantly by the activity of NPA-sensitive auxin efflux carriers (Delbarre et al., 1996). Our results reveal a major discrepancy between the concentration of NPA required to saturate the inhibition of auxin efflux (1 μM) and those reported to be necessary to inhibit either the BFA-sensitive cycling of PIN1 between the PM and an internal compartment (200 μM; Geldner et al., 2001), or PIN1 internalization in the *tir3* mutant of *BIG* (150 μM; Gil et al., 2001). These observations suggest that the stimulation of NAA accumulation in tobacco cells by NPA (Delbarre et al., 1996; Petrášek et al., 2002; this report) is unlikely to have resulted from perturbation of efflux carrier cycling. We show here that in suspension-cultured cells of BY-2 tobacco, the stimulation of NAA accumulation by NPA was markedly reversed at concentrations of NPA around 10 to 30 μM. In another tobacco cell line (VBI-0), although high concentrations of NPA (up to at least 100 μM) did not cause such a reversal, abnormalities in cell division and loss of cell polarity occurred at concentrations of NPA even as low as 10 μM (Petrášek et al., 2002). Therefore, at concentrations of NPA not much greater than those necessary to saturate auxin accumulation, both cell behavior and auxin transport may be perturbed by mechanisms that have nothing to do with the specific effects of NPA on the auxin efflux machinery.

The inhibitory effect of NPA on auxin efflux is extremely rapid. In the suspension-cultured tobacco cells used in our experiments, the stimulation of NAA accumulation by NPA occurred without measurable time lag. This indicates that in cell suspensions, in which NPA would be expected to reach binding sites very rapidly, the inhibitory effect of the compound on auxin efflux carrier activity is very fast. This rapid response contrasts with the rather long treatment periods used in the experiments of Geldner et al. (2001; 2 h) and of Gil et al. (2001; 3 h) to study the effects of NPA and BFA on PIN1 cycling and localization. Unfortunately, no information on the kinetics of the inhibitory effect of NPA on efflux carrier cycling was provided.

Consistent with its reported inhibitory effect on efflux carrier traffic to the PM (Delbarre et al., 1998; Morris and Robinson, 1998; Robinson et al., 1999; Geldner et al., 2001; see introduction), BFA also strongly promoted NAA accumulation by BY-2 cells in a concentration-dependent manner. However, as with NPA, high concentrations of BFA (above 30 μM) reversed the stimulation of auxin accumulation. This biphasic response is correlated with the action of BFA on the actin cytoskeleton (discussed below). In the cell suspensions used in our experiments, the maximum stimulation of NAA accumulation observed (22.7% after 20 min at 10 μM BFA) was substantially less than the maximum stimulation caused by NPA treatment (130.2% after 20 min at 1 μM). These results imply that although BFA may be effective in inhibiting membrane vesicle cycling, even under conditions where the response to BFA is maximal, a small proportion of carrier proteins continues to catalyze auxin efflux across the PM. Evidence for this possibility comes from the results of Geldner et al. (2001). These

Table I. *Summary of the effects of NPA (10–200 μM) and BFA (20–100 μM) on cell structures and auxin accumulation in suspension-cultured 2-d-old BY-2 tobacco cells*

Compound	Microtubules	Actin Filaments	Endoplasmic Reticulum	Auxin Accumulation
NPA	–[a]	–	–	+[b]
BFA	–	+	+	+

[a]–, No differences from control observed. [b]+, Structure affected and/or auxin accumulation increased.

authors demonstrated that treatment of Arabidopsis seedling roots with 50 μM BFA for 2 h resulted in internalization of PIN1. However, close examination of their Figure 1B illustrating this result (Geldner et al., 2001) suggests appreciable residual fluorescence in the PM from PIN1 markers.

BFA But Not NPA Affects the Cytoskeleton

Although a role for the cytoskeleton in polar auxin transport has been established (for review, see Muday, 2000), only few data are available on the state of AFs and MTs after disruption of polar auxin transport with inhibitors. Thus, we compared the effects of NPA and BFA on the arrangement and structure of the cytoskeleton under the same conditions as those used to study the effects of these compounds on NAA accumulation. In agreement with Saint-Jore et al. (2002), who reported that treatment of BY-2 cells with BFA did not affect cortical MTs and AFs, we also found no effect of BFA on cortical cytoskeletal components. However, in the perinuclear region we found that BFA caused actin to form prominent clusters. To our knowledge, this is the first report of this phenomenon in plants.

The lack of information about perinuclear actin possibly stems from the fact that most previous studies have concentrated on AFs in the cortical layer of cytoplasm, and the perinuclear region has largely been overlooked (compare with Satiat-Jeunemaitre et al., 1996; Saint-Jore et al., 2002). Recently, Waller et al. (2002) reported an increased membrane association of cortical actin and bundling of cortical AFs in maize epidermal cells after BFA treatment. This suggests that under some circumstances, even cortical actin can be modified by treatment with BFA. Because phalloidin (used here for actin cytoskeleton visualization) binds preferentially to F-actin, it is likely that the newly formed actin clusters produced in the perinuclear region consist of the filamentous form of actin. A possible explanation for the formation of the perinuclear actin clusters is that actin may play a role in the process of ER-Golgi apparatus fusion after BFA treatment (compare with Ritzenthaler et al., 2002).

The quantitative image analysis showed that perinuclear actin cluster formation increased with increasing concentrations of BFA up to 40 μM but declined substantially with further increase in BFA concentrations to 100 μM. A possible interpretation is that at high concentrations of BFA, the ER-Golgi hybrid compartment (Ritzenthaler et al., 2002) is not formed. As a consequence, AFs are unable to reorganize into clusters. The reduction in actin cluster formation at high BFA concentrations correlates with the reduced stimulation of NAA accumulation under the same conditions. One possibility is that the two processes are functionally connected.

In contrast to BFA, the phytotropin NPA did not cause any changes in the arrangement of either MTs or AFs at concentrations that clearly inhibit NAA transport. The lack of effect on the arrangement of MTs is consistent with similar observations by Hasenstein et al. (1999) on maize root cells, who found that the inhibition of auxin transport by NPA was not accompanied by changes in the orientation of cortical MTs. Several reports strongly point to an association of the NBP and F-AFs (Cox and Muday, 1994; Butler et al., 1998; Hu et al., 2000). Although this association seems essential for the inhibitory action of NPA on auxin efflux, the binding of NPA to the NBP appears not to disrupt the association of the NBP with the actin cytoskeleton (Hu et al., 2000; this report). Thus, we conclude that the inhibitory action of NPA on auxin efflux from plant cells is not associated with disruption of the cytoskeletal system.

BFA But Not NPA Affects the ER

To follow possible mechanisms underlying the changes in perinuclear actin organization, we also investigated the structure of ER in interphase BY-2 cells. Using cells expressing a fusion protein containing GFP and ER-signaling and ER-retention amino acid (His-Asp-Glu-Leu, HDEL) sequences, both mobile particles and a static polygonal network of tubules were observed as reported for other fusion proteins containing an HDEL retention signal (Boevink et al., 1996; Haseloff et al., 1997). Because proteins containing an HDEL retention sequence might occasionally escape from the ER to the cis-Golgi apparatus, where HDEL binds to a specific receptor (Boevink et al., 1998), the possibility cannot be excluded that the fluorescence signal could also be observed in the structure of the cis-Golgi. However, it is unlikely that the mobile particles seen in control cells in this study are Golgi stacks because they did not move in the stop and go fashion characteristic of Golgi stacks (Nebenführ et al., 1999). One possibility is that they are the small, dilated cisternae of ER described previously in Brassicaceae and tobacco guard cells by Hawes et al. (2001). Treatment of cells with BFA resulted in the appearance of brightly fluorescing static spots at the surface of the ER sheets. Similar results were reported by Boevink et al. (1999) and Batoko et al. (2000) for the transient expression of a GFP-HDEL-containing protein. These fluorescing spots may be accumulations of GFP in the ER, but a positive identification has not yet been made (C. Hawes, personal communication). The disintegration of the ER that was observed in our experiments is in agreement with results of Henderson et al. (1994), who showed disruption of ER after 3 h of treatment with BFA in maize root cells by immunofluorescence microscopy with anti-HDEL antibody. Ritzenthaler et al. (2002) reported that up to 20 min, treatment with BFA caused no visible alteration in ER morphology in BY-2 cells. Our results indicated that the first observable changes in ER-targeted GFP distribution

in BY-2 cells can be seen in as little as 5 min after BFA application, when disintegration of the tubular network and formation of fluorescent spots started.

In contrast to BFA treatments, NPA had no effect on ER-targeted GFP distribution in BY-2 cells. To our knowledge, no other data about phytotropin effects on ER are yet available.

The NPA Enigma

Geldner et al. (2001) reported that TIBA (and possibly also other auxin transport inhibitors) prevented the BFA-induced internalization of PIN1 and the traffic of internalized PIN1 to the PM after the BFA washout. Because similar effects of TIBA were observed on the cycling of a PM-ATPase and of the syntaxin KNOLLE, these authors suggested that auxin transport inhibitors affect auxin efflux by generally interfering with membrane trafficking processes. To generalize from these findings, however, may be premature, not least because TIBA is not a good representative of auxin transport inhibitors. First, TIBA does not fulfill the structural requirements of typical phytotropins and acts as a weak auxin antagonist (Katekar and Geissler, 1980). Although it inhibits auxin transport (Katekar and Geissler, 1980; Rubery, 1990), its high-affinity binding to maize microsomal preparations is only partially displaced by NPA (Depta et al., 1983), suggesting different loci of action of TIBA and phytotropins. Second, it has long been established that TIBA is itself a weak auxin, which unlike NPA, undergoes carrier-mediated polar transport on carriers that can be competed by IAA, 2,4-dichlorophenoxyacetic acid, and NAA (Depta and Rubery, 1984). Third, work in our laboratory has shown that in BY-2 tobacco cells, the stimulation of NAA accumulation (2 nM) is saturated by as little as 1 μM TIBA (H. Slizowska, M. Elčkner, and E. Zažímalová, unpublished data). Last, and more importantly, unlike NPA and IAA, at the concentration of 25 μM used by Geldner et al. (2001), TIBA causes substantial cytoplasmic acidification (Depta and Rubery, 1984). This, in turn, is likely to have nonspecific side effects on many cellular processes, possibly including secretory mechanisms.

We believe that there are other good reasons to be cautious in accepting the suggestion that auxin transport inhibitors act by generally interfering with vesicle traffic and turnover. The concentration of NPA stated to be necessary to bring about a similar reduction in PIN1 cycling to that caused by 25 μM TIBA (200 μM NPA; Geldner et al., 2001) is about two orders of magnitude greater than the concentration of NPA required to saturate inhibition of auxin efflux (1–3 μM; Petrášek et al., 2002; this report). Also, in suspension-cultured tobacco cells, concentrations of NPA exceeding about 50 μM reduce the stimulation of NAA accumulation substantially, possibly as a result of nonspecific side effects on the cells unrelated to the specific regulation of auxin efflux (Petrášek et al., 2002; this report). Finally, as discussed above, NPA has no effect on the arrangement of the cytoskeleton or ER in BY-2 cells, even at concentrations well above those that saturate the inhibition of auxin efflux. Therefore, NPA cannot inhibit actin-dependent vesicle traffic in general by an indirect action on the structure of the cytoskeleton and ER.

In conclusion, although the vesicle trafficking inhibitor BFA mimics some of the physiological effects of the phytotropin NPA, particularly insofar as they both inhibit carrier-mediated auxin efflux across the PM, our results clearly suggest that they do so by affecting different cellular mechanisms.

MATERIALS AND METHODS

Plant Material

Cells of tobacco (*Nicotiana tabacum* L. cv Bright-Yellow 2) line BY-2 (Nagata et al., 1992) were cultivated in darkness at 26°C on an orbital incubator (IKA KS501, IKA Labortechnik, Staufen, Germany; 120 rpm, orbital diameter 30 mm) in liquid medium (3% [w/v] Suc, 4.3 g L^{-1} Murashige and Skoog salts, 100 mg L^{-1} inositol, 1 mg L^{-1} thiamin, 0.2 mg L^{-1} 2,4-dichlorophenoxyacetic acid, and 200 mg L^{-1} KH_2PO_4 [pH 5.8]) and subcultured weekly. Stock BY-2 calli were maintained on media solidified with 0.6% (w/v) agar and subcultured monthly. Transgenic cells and calli were maintained on the same media supplemented with 100 μg mL^{-1} kanamycin and 100 μg mL^{-1} cefotaxim. All chemicals were obtained from Sigma (St. Louis) unless otherwise stated.

Transformation of BY-2 Cells

The basic transformation protocol of An (1985) was used. A 2-mL aliquot of 3-d-old BY-2 cells was co-incubated for 3 d with 100 μL of an overnight culture of *Agrobacterium tumefaciens* strain C58C1 carrying pBIN *m-gfp5*-ER plant binary vector (gift of Dr. Jim Haseloff, University of Cambridge, UK). It codes for ER-localized GFP variant mGFP5-ER, a thermotolerant derivative of mGFP4-ER (Haseloff et al., 1997), and contains a C-terminal ER retention signal sequence (HDEL). Incubated cells were then washed three times in 50 mL of liquid medium containing 100 μg mL^{-1} cefotaxim and plated onto solid medium containing 100 μg mL^{-1} kanamycin and 100 μg mL^{-1} cefotaxim. Kanamycin-resistant colonies appeared after 3 to 4 weeks of incubation in darkness at 27°C. Cell suspension cultures established from these were maintained as described above, with the addition of 100 μg mL^{-1} kanamycin and 100 μg mL^{-1} cefotaxim to the cultivation medium.

Effects of NPA and BFA on Cytoskeleton Arrangement

Appropriate volumes of a 25 mM stock solution of BFA in 96% (w/v) ethanol were added to cell cultures to give final concentrations of 20, 40, and 100 μM. NPA (synthesized in the Institute of Experimental Botany, Prague; compare with Petrášek et al., 2002) was added to cell cultures from 5 mM stock solution in 96% (w/v) ethanol to a final concentration of 50 μM (determined by reference to NPA concentration studies; see above). Equivalent volumes of 96% (w/v) ethanol were added to all control cultures.

Cell cultures were treated with BFA or NPA for 30 min with continuous shaking at room temperature (approximately 25°C) before microscopic examination (see below). When required, washout of BFA was performed with fresh cultivation medium after filtration of treated suspensions on 50-mm-diameter cellulose filter paper discs on a Nalgene filter holder (Nalge Company, Rochester, NY). Aliquots of 10 mL of cell suspension were washed three times (10 min each time) in 50 mL of fresh cultivation medium, and cells were examined immediately.

Visualization of AFs

AFs were visualized by the method of Kakimoto and Shibaoka (1987) modified according to Olyslaegers and Verbelen (1998). Filtered cells were fixed for 10 min in 1.8% (w/v) paraformaldehyde (PFA) in standard buffer (50 mM PIPES [pH 7.0], supplemented with 5 mM $MgCl_2$, and 10 mM EGTA). After a subsequent 10-min fixation in standard buffer containing 1% (v/v) glycerol, cells were rinsed twice for 10 min with standard buffer. Then, 0.5 mL of the resuspended cells were incubated for 35 min with the same volume of 0.66 μM TRITC-phalloidin prepared freshly from 6.6 μM stock solution in 96% (w/v) ethanol by dilution (1:10 [v/v]) in phosphate-buffered saline (PBS; 0.15 M NaCl, 2.7 mM KCl, 1.2 mM KH_2PO_4, and 6.5 mM Na_2HPO_4 [pH 7.2]). Cells were than washed three times for 10 min in PBS and observed immediately.

Visualization of MTs

MTs were visualized as described by Wick et al. (1981) with the modifications described by Mizuno (1992). After 30 min of prefixation in 3.7% (w/v) PFA in MT-stabilizing buffer consisting of 50 mM PIPES, 2 mM EGTA, and 2 mM $MgSO_4$ (pH 6.9) at 25°C, the cells were subsequently fixed in 3.7% (w/v) PFA and 1% (w/v) Triton X-100 in MT-stabilizing buffer for 20 min. After treatment with an enzyme solution (1% [w/v] macerozyme and 0.2% [w/v] pectinase) for 7 min at 25°C, the cells were attached to poly-L-Lys-coated coverslips and treated with 1% (w/v) Triton X-100 in MT-stabilizing buffer for 20 min. Subsequently, the cells were treated with 0.5% (w/v) bovine serum albumin in PBS and incubated with a monoclonal mouse antibody against α-tubulin (DM 1A, Sigma) for 45 min at 25°C (dilution 1:500 [v/v] in PBS). After washing with PBS, a secondary fluorescein isothiocyanate (FITC)-conjugated anti-mouse antibody (Sigma), diluted 1:80 (v/v) in PBS, was applied for 1 h at 25°C. Coverslips with cells were carefully washed in PBS, rinsed with water, and embedded in Mowiol solution (Polysciences, Warrington, PA).

Microscopy and Image Analysis

Both fixed and live preparations were observed with an epifluorescence microscope (Eclipse E600, Nikon, Tokyo) equipped with appropriate filter sets for FITC and TRITC fluorescence detection. mGFP5-ER fluorescence was observed using the FITC filter set. Images and time lapse scans were grabbed with a monochrome integrating CCD camera (COHU 4910, COHU Inc., San Diego) and digitally stored. The organization of both the cytoskeleton and ER were studied microscopically in at least 10 independent experiments. Representative images in Figures 3 and 5 show an arrangement typical for around 1,000 cells evaluated in each treatment. Subtle differences reflect the variability of staining pattern and appearance of cells.

After this careful microscopic examination, LUCIA image analysis software (Laboratory Imaging, Prague) was used for the evaluation of the effect of BFA on perinuclear actin aggregation. Images of TRITC-phalloidin-stained AFs were transformed to complementary colors (Fig. 4, A and C) and a circular measuring frame was applied interactively over the perinuclear region (Fig. 4, B and D). The ODV parameter was measured. The ODV parameter is the SD of optical density values under the circular measuring frame, where the bigger the ODV, the higher the aggregation of actin. These optical density values reflect the relative fluorescence intensities of individual pixels. The method measures the "coherency" of the fluorescent signal in the perinuclear region; the less coherent the signal, the greater the extent of actin aggregation. Approximately 300 cells in 10 optical fields were assessed for each sample.

Auxin Accumulation Measurement

Auxin accumulation by cells was measured according to the method of Delbarre et al. (1996), modified by Petrášek et al. (2002). The accumulation by the cells of [^{3}H]NAA (specific radioactivity 935 GBq $mmol^{-1}$, synthesized at the Isotope Laboratory, Institute of Experimental Botany, Prague), was measured in 0.5-mL aliquots of cell suspension (cell density about 7×10^5 cells mL^{-1}, as determined by counting cells in Fuchs-Rosenthal hemocytometer). Each cell suspension was filtered, resuspended in uptake buffer (20 mM MES, 40 mM Suc, and 0.5 mM $CaSO_4$, pH adjusted to 5.7 with KOH), and equilibrated for 45 min with continuous orbital shaking. Equilibrated cells were collected by filtration, resuspended in fresh uptake buffer, and incubated on the orbital shaker for 1.5 h in darkness at 25°C. [^{3}H]NAA was added to the cell suspension to give a final concentration of 2 nM. After a timed uptake period (depending on experiment, see above), 0.5-mL aliquots of suspension were withdrawn and accumulation of label was terminated by rapid filtration under reduced pressure on 22-mm-diameter cellulose filters. The cell cakes and filters were transferred to scintillation vials, extracted in ethanol for 30 min, and radioactivity was determined by liquid scintillation counting (Packard Tri-Carb 2900TR scintillation counter, Packard Instrument Co., Meriden, CT). Counts were corrected for surface radioactivity by subtracting counts obtained for aliquots of cells collected immediately after the addition of [^{3}H]NAA. Counting efficiency was determined by automatic external standardization, and counts were corrected automatically. NPA or BFA were added as required from ethanolic stock solutions to give the appropriate final concentration (see above). In time course experiments, aliquots of cell suspension were removed at timed intervals varying from 0 to 40 min from the start of experiments; the concentration dependence of auxin accumulation in response to NPA or BFA was determined after a 20-min uptake period.

Metabolism of Labeled Compounds

Possible distortion of the results of auxin accumulation studies by metabolism of the [^{3}H]NAA taken up by the cells was checked. Cells of BY-2 were incubated for 30 min as described in the presence of 2 nM [^{3}H]NAA. At the end of the incubation period, 10-mL aliquots of the incubated suspensions were quickly filtered on paper with gentle suction, washed rapidly with 5 mL of uptake buffer, and the cell cake was transferred to 2 mL of prechilled ethanol and stored at −80°C until required. Cell debris was removed by filtration under gentle pressure through cellulose filters. Radioactive compounds in the extracts were separated by chromatography on cellulose thin-layer plates (POLYGRAM CEL 300 UV_{254}, Macherey-Nagel, Düren, Germany), together with samples of the labeled auxins. The plates were developed in three independent solvent systems: (a) *iso*propanol:26% (v/v) ammonia:water (10:1:1 [v/v]), (b) chloroform:ethanol:glacial acetic acid (95:1:5 [v/v]), and (c) chloroform:ethanol:glacial acetic acid (75:20:5 [v/v]). Each chromatogram strip was cut into 20 sequential segments, eluted in ethanol, and counted by liquid scintillation counting.

ACKNOWLEDGMENTS

The authors thank Dr. Jim Haseloff (University of Cambridge, UK) for the pBIN *m-gfp5*-ER binary vector, and Miss Andrea Hourová (Institute of Experimental Botany, Prague) for her excellent technical assistance.

Received August 9, 2002; returned for revision September 10, 2002; accepted October 12, 2002.

LITERATURE CITED

An G (1985) High efficiency transformation of cultured tobacco cells. Plant Physiol **79:** 568–570

Batoko H, Zheng HQ, Hawes C, Moore I (2000) A Rab1 GTPase is required for transport between the endoplasmic reticulum and Golgi apparatus and for normal Golgi movement in plants. Plant Cell **12:** 2201–2217

Bennett MJ, Marchant A, Green HG, May ST, Ward SP, Millner PA, Walker AR, Schulz B, Feldmann KA (1996) *Arabidopsis AUX1* gene: a permease-like regulator of root gravitropism. Science **273:** 948–950

Bernasconi P, Patel BC, Reagan JD, Subramanian MV (1996) The *N*-1-naphthylphthalamic acid-binding protein is an integral membrane protein. Plant Physiol **111:** 427–432

Boevink P, Martin B, Oparka K, Santa Cruz S, Hawes C (1999) Transport of virally expressed green fluorescent protein through the secretory pathway in tobacco leaves is inhibited by cold shock and brefeldin A. Planta **208:** 392–400

Boevink P, Oparka K, Santa Cruz S, Martin B, Betteridge A, Hawes C (1998) Stacks on tracks: The plant Golgi apparatus traffics on an actin/ER network. Plant J **15:** 441–447

Boevink P, Santa Cruz S, Hawes C, Harris N, Oparka KJ (1996) Virus-mediated delivery of the green fluorescent protein to the endoplasmic reticulum of plant cells. Plant J **10:** 935–941

Butler JH, Hu SQ, Brady SR, Dixon MW, Muday GK (1998) In vitro and in vivo evidence for actin association of the naphthylphthalamic acid-binding protein from zucchini hypocotyls. Plant J **13:** 291–301

Cande WZ, Goldsmith MHM, Ray PM (1973) Polar auxin transport and auxin-induced elongation in the absence of cytoplasmic streaming. Planta **111:** 279–296

Cox DN, Muday GK (1994) NPA binding activity is peripheral to the plasma membrane and is associated with the cytoskeleton. Plant Cell **6:** 1941–1953

Davies PJ (1995) The plant hormone concept: concentration, sensitivity and transport. *In* PJ Davies, ed, Plant Hormones: Physiology, Biochemistry and Molecular Biology, Ed 2. Kluwer Academic Publishers, Dordrecht, The Netherlands, pp 13–38

Delbarre A, Muller P, Guern J (1998) Short-lived and phosphorylated proteins contribute to carrier-mediated efflux, but not to influx, of auxin in suspension-cultured tobacco cells. Plant Physiol **116:** 833–844

Delbarre A, Muller P, Imhoff V, Guern J (1996) Comparison of mechanisms controlling uptake and accumulation of 2,4-dichlorophenoxy acetic acid, naphthalene-1-acetic acid, and indole-3-acetic acid in suspension-cultured tobacco cells. Planta **198:** 532–541

Depta H, Eisele K-H, Hertel R (1983) Specific inhibitors of auxin transport: action on tissue segments and in vitro binding to membranes from maize coleoptiles. Plant Sci Lett **31:** 181–192

Depta H, Rubery PH (1984) A comparative study of carrier participation in the transport of 2,3,5-triiodobenzoic acid, indole-3-acetic acid, and 2,4-dichlorophenoxyacetic acid by *Cucurbita pepo* L. hypocotyl segments. J Plant Physiol **115:** 371–387

Dixon MW, Jacobson JA, Cady CT, Muday GK (1996) Cytoplasmic orientation of the naphthylphthalamic acid-binding protein in zucchini plasma membrane vesicles. Plant Physiol **112:** 421–432

Friml J, Palme K (2002) Polar auxin transport—old questions and new concepts? Plant Mol Biol **49:** 273–284

Gälweiler L, Guan C, Müller A, Wisman E, Mendgen K, Yephremov A, Palme K (1998) Regulation of polar auxin transport by AtPIN1 in *Arabidopsis* vascular tissue. Science **282:** 2226–2230

Geldner N, Friml J, Stierhof YD, Jürgens G, Palme K (2001) Auxin transport inhibitors block PIN 1 cycling and vesicle trafficking. Nature **413:** 425–428

Gil P, Dewey E, Friml J, Zhao Y, Snowden KC, Putterill J, Palme K, Estelle M, Chory J (2001) BIG: a calossin-like protein required for polar auxin transport in *Arabidopsis*. Genes Dev **15:** 1985–1997

Goldsmith MHM (1977) The polar transport of auxin. Annu Rev Plant Physiol **28:** 439–478

Haseloff J, Siemering KR, Prasher DC, Hodge S (1997) Removal of a cryptic intron and subcellular localisation of green fluorescent protein are required to mark transgenic *Arabidopsis* plants brightly. Proc Natl Acad Sci USA **94:** 2122–2127

Hasenstein KH, Blancaflor EB, Lee JS (1999) The microtubule cytoskeleton does not integrate auxin transport and gravitropism in maize roots. Physiol Plant **105:** 729–738

Hawes C, Saint-Jore C, Martin B, Zheng HQ (2001) ER confirmed as the location of mystery organelles in *Arabidopsis* plants expressing GFP! Trends Plant Sci **6:** 245–246

Henderson J, Satiat-Jeunemaitre B, Napier R, Hawes C (1994) Brefeldin A-induced disassembly of the Golgi apparatus is followed by disruption of the endoplasmic reticulum in plant cells. J Exp Bot **45:** 1347–1351

Hu SQ, Brady SR, Kovar DR, Staiger CJ, Clark GB, Roux SJ, Muday GK (2000) Identification of plant actin binding proteins by F-actin affinity chromatography. Plant J **24:** 127–137

Kakimoto T, Shibaoka H (1987) Actin filaments and microtubules in the preprophase band and phragmoplast of tobacco cells. Protoplasma **140:** 151–156

Katekar GF, Geissler AE (1980) Auxin transport inhibitors: IV. Evidence of a common mode of action for a proposed class of auxin transport inhibitors: the phytotropins. Plant Physiol **66:** 1190–1195

Li HM, Altschmied L, Chory J (1994) *Arabidopsis* mutants define downstream branches in the phototransduction pathway. Genes Dev **8:** 339–349

Lomax TL, Muday GK, Rubery PH (1995) Auxin transport. *In* PJ Davies, ed, Plant Hormones: Physiology, Biochemistry and Molecular Biology, Ed 2. Kluwer Academic Publishers, Dordrecht, The Netherlands, pp 509–530

Luschnig C (2001) Auxin transport: why plants like to think BIG. Curr Biol **11:** 831–833

Mizuno K (1992) Induction of cold stability of microtubules in cultured tobacco cells. Plant Physiol **100:** 740–748

Morris DA (2000) Transmembrane auxin carrier systems—dynamic regulators of polar auxin transport. Plant Growth Regul **32:** 161–172

Morris DA, Robinson JS (1998) Targeting of auxin carriers to the plasma membrane: differential effects of brefeldin A on the traffic of auxin uptake and efflux carriers. Planta **205:** 606–612

Morris DA, Rubery PH, Jarman J, Sabater M (1991) Effects of inhibitors of protein synthesis on transmembrane auxin transport in *Cucurbita pepo* L. hypocotyl segments. J Exp Bot **42:** 773–783

Müller A, Guan CH, Gälweiler L, Tänzler P, Huijser P, Marchant A, Parry G, Bennett M, Wisman E, Palme K (1998) *AtPIN2* defines a locus of *Arabidopsis* for root gravitropism control. EMBO J **17:** 6903–6911

Muday GK (2000) Maintenance of asymmetric cellular localization of an auxin transport protein through interaction with the actin cytoskeleton. J Plant Growth Regul **19:** 385–396

Muday GK, DeLong A (2001) Polar auxin transport: controlling where and how much. Trends Plant Sci **6:** 535–542

Muday GK, Murphy AS (2002) An emerging model of auxin transport regulation. Plant Cell **14:** 293–299

Nagata T, Nemoto Y, Hasezava S (1992) Tobacco BY-2 cell line as the "Hela" cell in the cell biology of higher plants. Int Rev Cytol **132:** 1–30

Nebenführ A, Gallagher LA, Dunahay TG, Frohlick JA, Mazurkiewicz AM, Meehl JB, Staehelin LA (1999) Stop-and-go movements of plant Golgi stacks are mediated by the acto-myosin system. Plant Physiol **121:** 1127–1141

Olyslaegers G, Verbelen JP (1998) Improved staining of F-actin and co-localization of mitochondria in plant cells. J Microsc Oxford **192:** 73–77

Petrášek J, Elčkner M, Morris DA, Zažímalová E (2002) Auxin efflux carrier activity and auxin accumulation regulate cell division and polarity in tobacco cells. Planta **216:** 302–308

Raven JA (1975) Transport of indoleacetic acid in plant cells in relation to pH and electrical potential gradients, and its significance for polar IAA transport. New Phytol **74:** 163–174

Richards S, Hillman T, Stern M (1996) Mutations in the *Drosophila* push-over gene confer increased neuronal excitability and spontaneous synaptic vesicle fusion. Genetics **142:** 1215–1223

Ritzenthaler C, Nebenführ A, Movafeghi A, Stussi-Garaud C, Behnia L, Pimpl P, Staehelin LA, Robinson DG (2002) Reevaluation of the effects of brefeldin A on plant cells using tobacco bright yellow 2 cells expressing Golgi-targeted green fluorescent protein and COPI antisera. Plant Cell **14:** 237–261

Robinson JS, Albert AC, Morris DA (1999) Differential effects of brefeldin A and cycloheximide on the activity of auxin efflux carriers in *Cucurbita pepo* L. J Plant Physiol **155:** 678–684

Rubery PH (1990) Phytotropins: receptors and endogenous ligands. Symp Soc Exp Biol **44:** 119–146

Rubery PH, Sheldrake AR (1974) Carrier-mediated auxin transport. Planta **188:** 101–121

Ruegger M, Dewey E, Hobbie L, Brown D, Bernasconi P, Turner J, Muday G, Estelle M (1997) Reduced naphthylphthalamic acid binding in the *tir3* mutant of Arabidopsis is associated with a reduction in polar auxin transport and diverse morphological defects. Plant Cell **9:** 745–757

Satiat-Jeunemaitre B, Steele C, Hawes C (1996) Golgi-membrane dynamics are cytoskeleton dependent: a study on Golgi stack movement induced by brefeldin A. Protoplasma **191:** 21–33

Saint-Jore CM, Evins J, Batoko H, Brandizzi F, Moore I, Hawes C (2002) Redistribution of membrane proteins between the Golgi apparatus and endoplasmatic reticulum in plants is reversible and not dependent on cytoskeletal networks. Plant J **29:** 661–678

Sussman MR, Gardner G (1980) Solubilization of the receptor for *N*-1-naphthylphthalamic acid. Plant Physiol **66:** 1074–1078

Swarup R, Friml J, Marchant A, Ljung K, Sandberg G, Palme K, Bennett M (2001) Localization of the auxin permease AUX1 suggests two functionally distinct hormone transport pathways operate in the *Arabidopsis* root apex. Genes Dev **15:** 2648–2653

Waller F, Riemann M, Nick P (2002) A role of actin-driven secretion in auxin-induced growth. Protoplasma **219:** 72–81

Wick SM, Seagull RW, Osborn M, Weber K, Gunning BES (1981) Immunofluorescence microscopy of organized microtubule arrays in structurally stabilized meristematic plant cells. J Cell Biol **89:** 685–690

Wilkinson S, Morris DA (1994) Targeting of auxin carriers to the plasma membrane: effects of monensin on transmembrane auxin transport in *Cucurbita pepo* L. tissue. Planta **193:** 194–202